

AN APPROACH TO APPLICATION VALIDATION OF MULTISPECTRAL SENSORS USING AVIRIS DATA

Amanda Warner*, Slawomir Blonski*, Gerald Gasser*, Robert Ryan*, and Vicki Zanoni**

1. INTRODUCTION

High spatial resolution multispectral/hyperspectral sensors are being developed by private industry with science/research customers as end users. With an increasingly wide range of sensor choices, it is important for the remote sensing science community and commercial community alike to understand the trade-offs between ground sample distance (GSD), spectral resolution, and signal-to-noise ratio (SNR) in selecting a sensor that will best meet their needs. High spatial resolution hyperspectral imagery and super resolution multispectral charge-coupled device imagery can be used to develop prototypes of proposed data acquisition systems without building new systems or collecting large sets of additional data. By using these datasets to emulate proposed and existing systems, imaging systems may be optimized to meet customer needs in a virtual environment. This approach also enables one to determine, a priori, whether an existing dataset will be useful for a given application.

NASA's Earth Science Applications Directorate at the John C. Stennis Space Center (SSC) supports state and local governments, commercial companies, agricultural-related users, and researchers: all of whom have finite financial resources. The Applications Directorate assists these organizations, which in some cases have no background in remote sensing science, in selecting the imagery that will best meet their needs. The need to simulate other sensors lies in the tradespace between cost and utility. The number of pixels, number of bands, spectral coverage, and SNR all drive the cost of conducting an image survey. When planning a mission, the altitude of the plane can have serious coverage, cost, and usefulness impacts. While it might be less costly to fly higher and to cover a larger area, the subsequent data might not carry the information needed to make informed decisions.

In this study, we performed spatial synthesis and spectral integration, and we applied noise to AVIRIS-LA (low altitude) imagery to parametrically simulate the performance of example sensors. AVIRIS data were selected as the source data to use in these simulations because of the system's high SNR, excellent radiometric performance, and very high spatial and spectral resolution. With these characteristics, we may simulate larger GSD, lower SNR, and lower spectral resolutions by aggregating pixels, by binning spectral bands, and by adding random noise. AVIRIS data may also be used to more fully understand the limitations of spaceborne hyperspectral systems. The recent launch of the Hyperion hyperspectral instrument on the EO-1 platform has served to reinforce the fact that although hyperspectral instruments are finally making it into space, spatial resolution and SNR are not at the level of airborne hyperspectral sensors. For scientific usage, the limitations and advantages of these sensors need to be understood.

As aerial and satellite systems evolve, both the government and the private sector will benefit from improved requirements analysis. A preliminary set of tools now exists to address many related questions. Previous studies have examined the impact of GSD, spectral resolution, and noise on hyperspectral image analysis (Table 1). Our approach was to develop a set of tools that creates simulated datasets from AVIRIS-LA and that will parametrically vary GSD, spectral resolutions, noise characteristics, and additional platform characteristics to better understand the utility of present and planned commercial systems. The Applications Research Toolbox currently in development at SSC will be used in collaboration with industry partners to help define future systems. This paper demonstrates some of the technology that will be present in this toolbox and performs preliminary analysis on simulation metrics.

* Lockheed Martin Space Operations – Stennis Programs, John C. Stennis Space Center (Principal contact: Robert.Ryan@ssc.nasa.gov)

** National Aeronautics and Space Administration, John C. Stennis Space Center

Table 1. Previous studies on the impact of GSD, spectral resolution, and noise on hyperspectral image analysis.

Impact Factor	Previous Studies
GSD	Green and Boardman, 2000; Kruse, 2000; Perry et al., 2000; Smailbegovic et al., 2000; Chabrilat and Goetz, 1999; Goetz and Kindel, 1999; Rockwell et al., 1999; Shen, 1997; Teillet et al., 1997; Goetz and Kindel, 1996; Price, 1997; Justice et al., 1989.
Spectral Resolution	Asner and Heidebrecht, in press; Boardman and Green, 2000; Kruse, 2000; Warner et al., 2000; Kokaly and Clark, 1999; Price, 1997; Shen, 1997; Teillet et al., 1997; Swayze and Clark, 1995.
Noise	Green and Boardman, 2000; Kruse, 2000; Okin and Roberts, 2000; Goetz and Kindel, 1999; Kokaly and Clark, 1999; Shen, 1997; Clark and Swayze, 1996; Swayze and Clark, 1995; Curran et al., 1991.

2. METHODS

2.1 Simulation

We began our simulation process by selecting an image that represented a wide variety of landcover to observe the results of simulation on a variety of surface features. The primary site selected was a subscene of 1999 AVIRIS-LA Yellowstone National Park imagery. This scene contains riparian features, roads, exposed soil, senesced and live vegetation, and water. The first step in the simulation process was to use the scale factors provided by the AVIRIS team to bring the data into non-scaled radiance units. Although this step is not necessary for all processing scenarios, using radiometric units does allow the user the option of comparing the finalized simulation product to other data sources if desired. Following this step, the data were either kept at the original AVIRIS wavelengths or mapped to the Landsat ETM+ channels by integrating the AVIRIS data over the ETM+ filter response functions. Landsat ETM+ filter response functions were used in these simulations because many commercial and government systems use similar bands. The next step after spectral resampling was spatial aggregation. Pixels were aggregated in this study through block averaging using the IDL routine *rebin*. Pixels were scaled by 5, 10, 15, and 20 times the original resolution. See Figure 1 for processing flow.

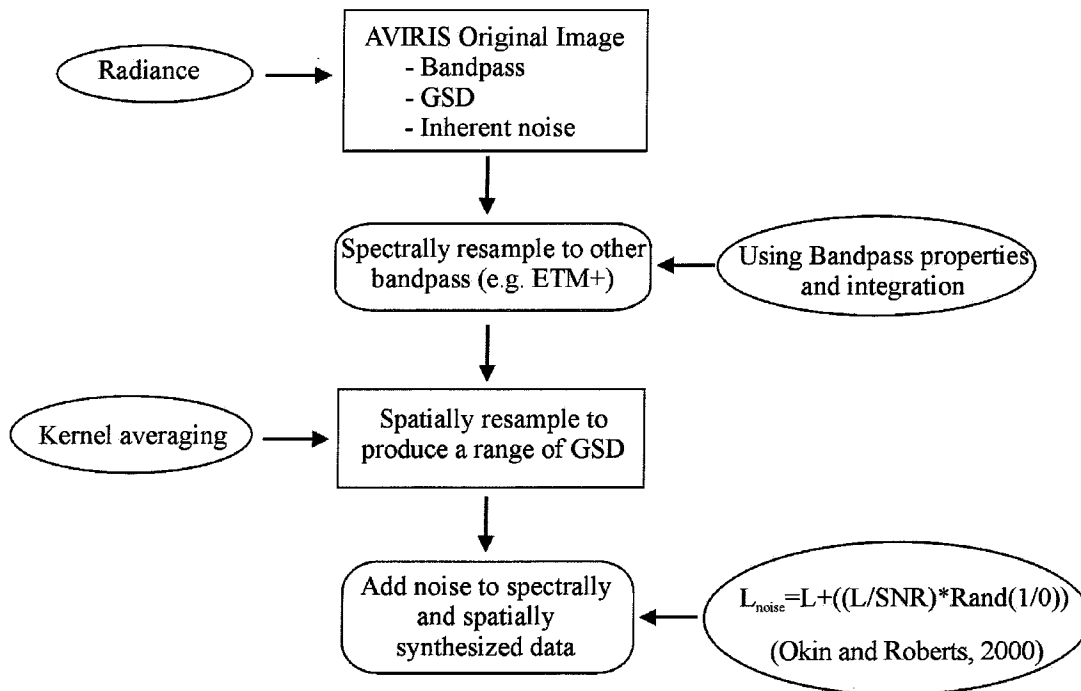


Figure 1. Flowchart of simulation process.

The last step prior to analysis was to add random noise to the dataset to simulate various SNR levels. This step was performed using equation 1 from Okin and Roberts (2000):

$$L(\lambda)_{\text{noise}} = L(\lambda) + ((L(\lambda)/\text{SNR}) * \text{Rand}(1/0)) \quad (1)$$

Where:

L_{noise}	=	Resulting radiance with noise added
L	=	Original radiance values with system inherent noise
SNR	=	Signal to noise value used; i.e., 100, 25 etc.
$\text{Rand}(1/0)$	=	Normally distributed random number with a mean of zero and a standard deviation of 1.

This method applies noise that is based on the radiance of each band but does not include detector-specific noise characteristics. The above expression is valid when the input scene SNR is much higher than the simulated SNR. This approach adds random noise without separating the individual sources of noise, which holds after spatial and spectral integration.

2.2 Noise Considerations

Sensor designs often must incorporate tradeoffs between SNR and GSD. Decreasing the GSD without compensating the optical throughput (i.e., lengthening the telescope and narrowing the aperture to achieve a smaller GSD) will reduce the SNR. In other words, for a fixed telescope diameter and detector size, the number of photons reaching the detector for a smaller GSD will be reduced and the SNR will be lower. Improving the spatial resolution may result in poor quality but high spatial resolution data. Most systems are limited by a combination of photon and detector noise. For our simulations, we simply added random (Poisson) noise, which accounts for both of these processes. Sources of coherent noise, such as striping and power supply noise, were not considered here but might be selected for simulation in the Application Research Toolbox.

2.3 Simulated Product Assessment

Following the simulation process, the data were displayed to examine visual effects from the synthesis. The images were transformed into eigenspace to appraise the effects of the simulation on eigenvectors. Principal Component Analysis (PCA) or eigen analysis is a routine widely used to assess the variance of an image. Image bands are orthogonally projected to determine axes of maximum variance. The coefficients to rotate each band into these new axes are the eigenvectors. Eigenvectors are ranked in order of maximum variance (the first principal component) to the dimension of least variance (the last component). PCA results can be used as input into classifiers because some surface features are more apparent when taken into PC space. The appearance of noise in eigenvectors is indicative of reduced data dimensionality. By looking at the eigenvectors of degraded data, we can see when noise and spatial resolution begin to change the dimensionality of an image relative to the original dataset.

3. RESULTS

Normalized Difference Vegetation Index (NDVI) was computed using the simulated images to show the effects of the reduced spatial resolution. While this step is quite simple, the product can have a large impact on users who need to determine the GSD necessary to observe phenomena. Evaluating the effects of various GSD on NDVI can aid in the development of the user's spatial requirements for applications such as precision agriculture. In Figure 2, it is clear that while 17.0 m images still show the road and features of the creek, the utility of these images for geographic information system work would be limited compared to the utility of the 8 m images, where feature boundaries are more defined. For example, Warfighter/Orbview 4 might be able to detect features spatially where Hyperion would not. A simulated product such as this would be valuable to users whose imagery can be acquired at varying altitudes to determine how GSD affects their ability to resolve surface features of interest.

Eigenvector analysis proved to be very useful for determining the effects of noise and degraded spatial resolution. While the NDVI images with 100:1 signal to noise added do not visually look different than the images with higher SNR, the eigenvectors with higher noise levels clearly show how noise influences the dimensionality of an image (see Figure 3, panel c, eigenvectors 9 and 10). When eigenvectors are no longer coherent and are

dominated by noise, the subsequent rotation of the original image by the noisy eigenvector is a noisy PC image that shows little about the original scene. When higher-order eigenvectors are not dominated by noise, the subsequent image data from the rotation can be used to identify more spectrally subtle features. The effect of lower SNR on dimensionality has been studied with historical AVIRIS data (Kruse, 2000). Through eigen analysis we can observe the effects of SNR on proposed systems and determine at what noise level features of interest are lost.

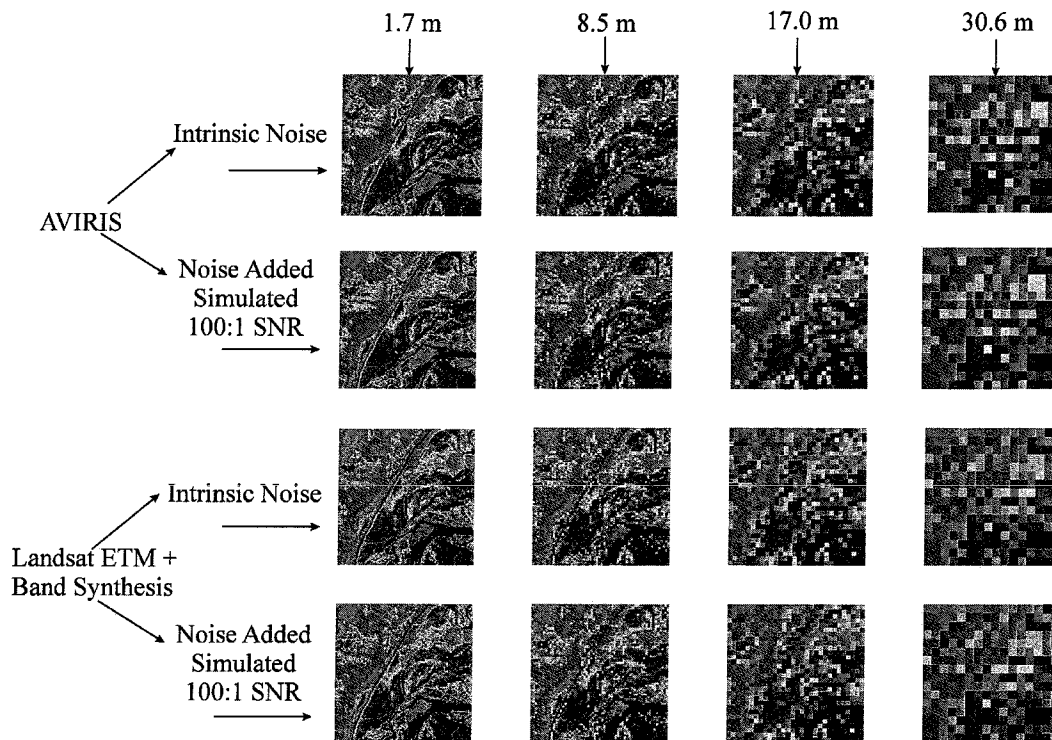


Figure 2. NDVI images with varying spatial resolution, spectral resolution, and noise levels. Visually, spatial resolution is more important than SNR when SNR for NDVI bands is greater than or equal to 100:1.

The eigenvector plots of Figure 3 also show that while noise reduces the dimensionality of a scene, larger GSD changes the shape of high-order eigenvectors. Starting with the fourth eigenvector for all noise levels, the shape of the eigenvectors for all increased GSD departs from that of the original spatial resolution. This change shows that although noise levels influence the dimensionality, the spatial resolution can greatly affect the type of information that may be extracted from the image. The coefficients for rotation would be changed and the eigenvectors with larger GSD would highlight different materials. These results are significant to researchers and commercial users alike who have several options for GSD to accomplish their mapping objective. Using eigen analysis enables visualization of the noise levels and spatial resolution where the detection of scene components is diminished.

We also performed noise addition and eigen analysis on the spectrally synthesized AVIRIS data (Figure 4). AVIRIS data were mapped to Landsat ETM+ filter response functions in this scenario. The results from this process are not as intriguing in respect to dimensionality as were the hyperspectral data because of the greatly reduced number of bands. The eigenvectors from the mapped data do show that with larger spectral resolution, the effects of noise and reduced GSD are not as noticeable in principal component analysis. The second eigenvector of the simulated data departs from the shape of the original resolution eigenvector at all noise levels. The PC images for this eigenvector are shown in Figure 5. Although the eigenvectors for the 2nd principal component are different, the overall shape is preserved and similar features are highlighted in the PC image. Lowered SNR and reduced spatial resolution do not affect eigenvectors as much with multispectral data as with hyperspectral data.

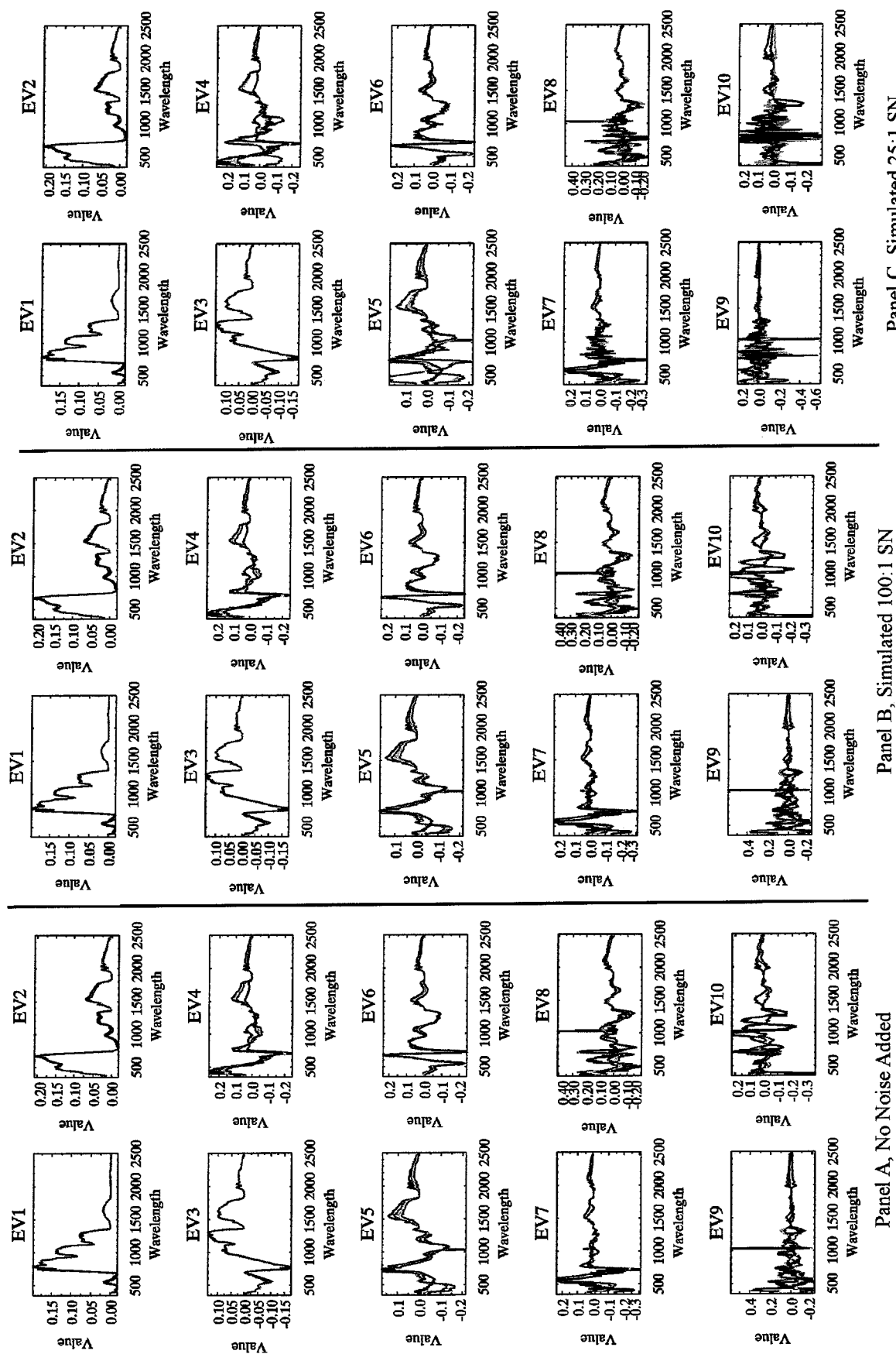
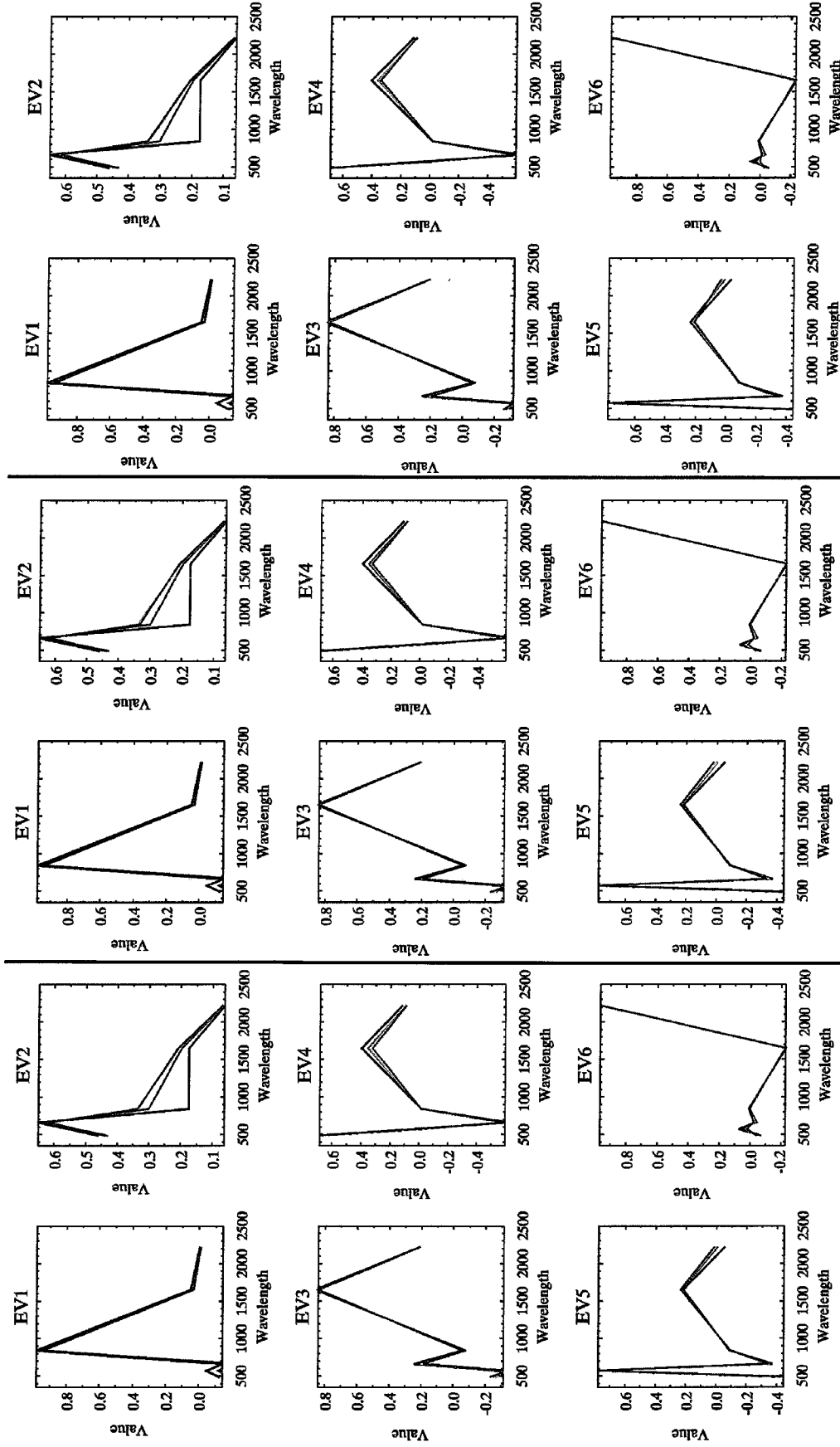


Figure 3. Eigenvectors for spatial resolutions of 1.7 m —, 17 m —, 25.5 m —, and 34 m —; noise levels are indicated beneath each panel.



Panel C, Simulated 25:1 SN

Panel B, Simulated 100:1 SN

Panel A, No Noise Added

Figure 4. Landsat ETM+ spectral resolution eigenvectors for spatial resolutions of 1.7 m—, 25.5 m—, 17 m—, and 34 m—; noise levels are indicated beneath each panel.

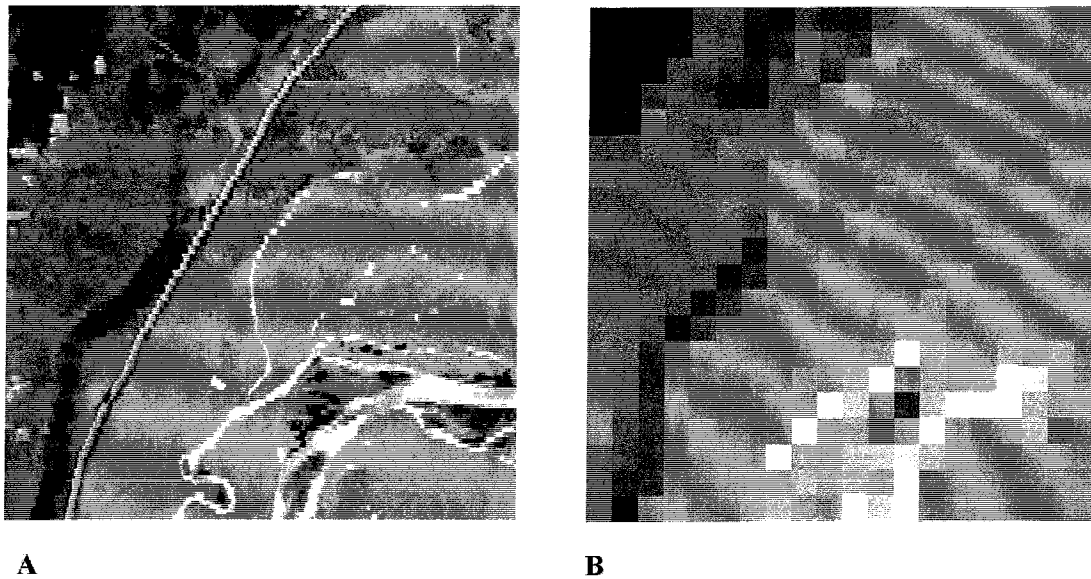


Figure 5. Landsat ETM+ convolved 2nd PC bands.

Figure 5a is the 2nd PC band of the scene convolved to Landsat ETM+ bands with no additional noise added and at the original spatial resolution. Figure 5b is the 2nd PC band of Landsat convolved data at 25.5-m spatial resolution with no noise added. The departure seen in the second eigenvector in Figure 5 is difficult to attribute to a surface feature since the very dark and very light areas in each scene correspond to each other. The departure is most likely related to spatial degradation's diluting the intensity of components.

4. CONCLUSIONS

Simulations produced by parametrically varying GSD show that SNR of 100:1 might not visually affect results (e.g., NDVI), but its effects can be better quantified by looking at eigenvectors. Changes observed in eigenvectors shapes at lower SNR are more due to spatial effects than added noise. This result is significant and should be investigated for a variety of scenes to determine the effects of spatial dilution on principal components. Continued work is needed to develop more robust noise models that will more realistically include the multiple sources of noise found in aircraft and satellite imagery as well as the overall level. Further analysis of the spatial properties of images could be analyzed as well for the contribution that the point-spread function of a sensor plays in principal component analysis. We hope to further parameterize these simulations to fit future and present systems in an effort to show the effects of data characteristics on applications. As both aerial and satellite systems evolve, both the government and the private sector will benefit from improved requirements analysis. A preliminary set of tools now exists to address this issue. Analysis will continue to define the "right questions" and to develop relevant metrics for data evaluation.

5. ACKNOWLEDGEMENTS

The authors wish to thank Greg Terrie for his helpful review of this paper as well as Marcia Wise, Lee Estep, Joe Spruce, and Judith Berglund for helpful comments along the way. This research was supported by the NASA Earth Science Applications Directorate under contract number NAS 13-650 at the John C. Stennis Space Center, Mississippi.

6. REFERENCES

Asner, G. P., and K. B. Heidebrecht, in press, "Spectral Unmixing of Vegetation, Soil and Dry Carbon Cover in Arid Regions: Comparing Multispectral and Hyperspectral Observations," *International Journal of Remote Sensing*.

Boardman, J. W., and R. O. Green, 2000, "Exploring the Spectral Variability of the Earth as Measured by AVIRIS in 1999," 2000 Proceedings from the Airborne Earth Science Workshop, JPL Publication, online at http://makalu.jpl.nasa.gov/docs/workshops/00_docs/Boardman_web.pdf.

Chabrilat, S. and A. F. H. Goetz, 1999, "The Search for Swelling Clays Along the Colorado Front Range: The Role of AVIRIS Resolution in Detection," 1999 Proceedings from the Airborne Earth Science Workshop, JPL Publication CHA-1-CHA-11, online at http://makalu.jpl.nasa.gov/docs/workshops/00_docs/Boardman_web.pdf.

Clark, R. N., and G. A. Swayze, 1996, "Evolution in Imaging Spectroscopy Analysis and Sensor Signal-to-noise: An Examination of How Far We Have Come," 1996 Proceedings from the Airborne Earth Science Workshop, JPL Publication 49-53, online at http://makalu.jpl.nasa.gov/docs/workshops/96_docs/7.PDF.

Curran, P. J., J. L. Dungan, and G. M. Smith, 1991, "Increasing the Signal-to-Noise Ratio of AVIRIS Imagery Through Repeated Sampling," 1991 Proceedings from the Airborne Geoscience Workshop, JPL Publication, online at http://makalu.jpl.nasa.gov/docs/workshops/91_docs/22.PDF.

Goetz, A. F. H., and B. Kindel, 1999, "Comparison of Unmixing Results Derived from AVIRIS, High and Low Resolution, and HYDICE images at Cuprite, NV," 1999 Proceedings from the Airborne Earth Science Workshop, JPL Publication GOE-1—GOE-9, online at http://makalu.jpl.nasa.gov/docs/workshops/99_docs/25.pdf.

Goetz, A. F. H., and B. Kindel, 1996, "Understanding Unmixed AVIRIS Images in Cuprite, NV Using Coincident HYDICE Data," 1996 Proceedings from the Airborne Geoscience Workshop, JPL Publication 97-103, online at http://makalu.jpl.nasa.gov/docs/workshops/96_docs/15.PDF.

Green, R. O., and J. W. Boardman, 2000, "Exploration of the Relationship Between Information Content and Signal-to-noise Ratio and Spatial Resolution in AVIRIS Spectral Data," 2000 Proceedings from the Airborne Earth Science Workshop, JPL Publication, online at http://makalu.jpl.nasa.gov/docs/workshops/00_docs/Green_Explor_web.pdf.

Justice, C. O., B. L. Markham, J. R. E. Townsend, and R. L. Kennard, 1989, "Spatial Degradation of Satellite Data," *International Journal of Remote Sensing*, 10:1539-1561.

Kokaly, R. F., and R. N. Clark, 1999, "Spectroscopic Determination of Leaf Biochemistry Using Band-depth Analysis of Absorption Features and Stepwise Linear Regression," *Remote Sensing of Environment*, 67:267-287.

Kruse, F. A., 2000, "The Effects of Spatial Resolution, Spectral Resolution, and Signal-to-noise Ratio on Geologic Mapping Using Hyperspectral Data, Northern Grapevine Mountains, Nevada," 2000 Proceedings from the Airborne Earth Science Workshop, JPL Publication, online at http://makalu.jpl.nasa.gov/docs/workshops/00_docs/Kruse_web.pdf.

Okin, G. S., and D. A. Roberts, 2000, "Linear Unmixing of Simulated, Noisy Spectra: Vegetation Detection Limits in Areas of Low Cover," 2000 Proceedings from the Airborne Earth Science Workshop, JPL Publication, online at http://makalu.jpl.nasa.gov/docs/workshops/00_docs/orkin_web.pdf.

Perry, E. M., M. Gardener, J. Tagestad, D. Roberts, P. Cassady, J. Smith, and D. Nichols, 2000, "Effects of Image Resolution and Uncertainties on Reflectance-derived Crop Stress Indicators," 2000 Proceedings from the Airborne Earth Science Workshop, JPL Publication, online at http://makalu.jpl.nasa.gov/docs/workshops/00_docs/perry_web.pdf.

Price, J. C., 1997, "Spectral Band Selection for Visible-Near Infrared Remote Sensing: Spectral-Spatial Resolution Tradeoffs," *IEEE Transactions on Geoscience and Remote Sensing*, 35(5):1277-1285.

Rockwell, B. W., R. N. Clark, K. E. Livo, R. R. McDougal, R. F. Kokaly, and J. S. Vance, 1999, "Preliminary Materials Mapping in the Park City Region for the Utah USGS-EPA Imaging Spectroscopy Project Using Both High and Low Altitude AVIRIS Data," 1999 Proceedings from the Airborne Geoscience Workshop, JPL Publication, online at http://makalu.jpl.nasa.gov/docs/workshops/99_docs/51.pdf.

Shen, S. S., 1997, "Multiband Sensor System Design Tradeoffs and Their Effects on Remote Sensing and Exploitation," SPIE Imaging Spectrometry III, 3118:296-307.

Smailbegovic, A., J. V. Taranik, and F. Kruse, 2000, "Importance of Spatial and Radiometric Resolution of AVIRIS Data for Recognition of Mineral Endmembers in the Geiger Grade Area, Nevada, U.S.A.," 2000 Proceedings from the Airborne Geoscience Workshop, JPL Publication, online at http://makalu.jpl.nasa.gov/docs/workshops/00_docs/smailbegovic_web.pdf.

Swayze, G. A., and R. N. Clark, 1995, "Spectral Identification of Minerals Using Imaging Spectrometry Data: Evaluating the Effects of Signal to Noise and Spectral Resolution Using the Tricorder Algorithm," 1995 Proceedings from the Airborne Geoscience Workshop, JPL Publication, online at http://makalu.jpl.nasa.gov/docs/workshops/95_docs/42.PDF.

Teillet, P. M., K. Staenz, and D. J. Williams, 1997, "Effects of Spectra, Spatial, and Radiometric Characteristics on Remote Sensing Vegetation Indices of Forested Regions," Remote Sensing of Environment 61:139-149.

Warner, A. S., A. F. H. Goetz, K. B. Heidebrecht, and E. L. Johnson, 2000, "Measuring the Ability of Landsat 7 to Map Vegetative Fractions Using a Near-simultaneous AVIRIS Underflight," 2000 Proceedings from the Airborne Earth Science Workshop, JPL Publication, online at http://makalu.jpl.nasa.gov/docs/workshops/00_docs/warner_web.pdf.